frontiers in Materials

ORIGINAL RESEARCH
published: 13 December 2021
doi: 10.3389/fmats.2021.788079

Study on Metakaolin Impact on Concrete Performance of Resisting Complex Ions Corrosion

Chen Xupeng[1]*, *Sun Zhuowen*[2] and *Pang Jianyong*[1]

[1]School of Civil Engineering and Architecture, Anhui University of Science and Engineering, Huainan, China, [2]School of Transportation and Civil Engineering, Nantong University, Nantong, China

The main purpose of this study is to determine the metakaolin (MK) impacts on the concrete durability when the concrete is subjected to joint corrosion of SO_4^{2-},Mg^{2+} and, Cl^-. Four groups of concrete test samples, which contained different MK contents, were designed and tested in order to see their physical property changes and macro-morphology differences during the cyclic corrosion process. And a series of approaches, including XRD, FTIR, SEM, and EDS, were applied to study the concrete phase composition changes and the micro-morphology features of all groups. According to the test results, when reaching 20 cycles, the concrete sample with 10% MK showed the best concrete physical properties; when reaching 120 cycles, the concrete with 5% MK content showed the best durability, produced similar amount of corrosion products to ordinary concrete, and presented relatively compacted micro-structure and small internal porosity. Mg^{2+} actually has a great impact on metakaolin. The corrosion product quantity increased significantly when MK admixture reached 15%. Due to the great number of produced M-S-H, the corrosive ions damaged the concrete for a second time, leading to serious aggregate peeling-off, powder surface of test samples, and porous micro-structure.

Keywords: concrete, metakaolin, dry-wet alternation, ion corrosion, micro-analysis

OPEN ACCESS

Edited by:
Dake Xu,
Northeastern University, China

Reviewed by:
Jie Hu,
South China University of Technology, China
Yang Zhou,
Southeast University, China

***Correspondence:**
Chen Xupeng
1933310001@stmail.ntu.edu.cn

Specialty section:
This article was submitted to "Structural Materials", a section of the journal Frontiers in Materials

Received: *04 October 2021*
Accepted: *15 November 2021*
Published: *13 December 2021*

Citation:
Xupeng C, Zhuowen S and Jianyong P (2021) Study on Metakaolin Impact on Concrete Performance of Resisting Complex Ions Corrosion. Front. Mater. 8:788079. doi: 10.3389/fmats.2021.788079

INTRODUCTION

With the rapid development of economy and continuous improvement of industrialization, large infrastructures, such as high-rise buildings, large bridges, and tunnels, have been constructed one after another. However, behind the huge economic benefits brought by the above-mentioned infrastructures, there is a great concern about the environmental pollution and energy consumption (Bildirici, 2019). The carbon dioxide (CO_2) produced due to cement production accounts for 8% of total CO_2 emission of the whole globe (Xi et al., 2016; Andrew, 2019). And for the reduction of greenhouse gas emission of the cement industry around the world, the most effective way is to minimize the cement use (Environment et al., 2018), which can be achieved by replacing certain proportion of cement by mineral admixture. Both the coal fly ash and blast furnace slag are the commonly used mineral admixtures (Supit and Shaikh, 2014; Juenger and Siddique, 2015; Hemalatha and Ramaswamy, 2017), but for common coal fly ash, though it can effectively reduce cement dosage and lower the economic cost, it has adverse effect on concrete performance at initial stage due to its low activity and large particle size (Jiang, 2005).

Metakaolin is a highly active pozzolanic material, which is produced by mineral resource of Kaolin burnt in 500–900°C temperature. Kaolin actually spreads widely with rich reserves around the

world. Taking China for instance, Kaolin reserve reaches 3 billion tons, among which, 3/4 hasn't been exploited and utilized. And this data only ranks fifth in the globe (Zhang et al., 2021a). The pozzolanic activity of metakaolin is even higher than silica fume (Wei et al., 2019), so that the metakaolin can engage in secondary reaction with $Ca(OH)_2$ during hydration process to produce large amount of C-S-H, as well as hydrated calcium aluminate and calcium sulphoaluminate hydrate. The hydration products can reduce the porosity of the concrete (Jiang et al., 2015), and enhance the cementious capability of the aggregates and the slurry (Mo et al., 2020). Zeng et al.(2014) believed that the metakaolin can reduce the pores in mortar, thereby refining the pore diameter inside the mortar. Besides, the metakaolin can also improve the mechanical properties of the concrete at the initial stage (Chen et al., 2021a), which perfectly solve the adverse effects brought by traditional mineral admixture (ordinary coal fly ash and blast furnace slag) to the concrete.

Sulfate has always been a key environmental factor that can seriously damage the concrete from both chemical and salt crystallization aspects. The chemical corrosion is represented by the SO_4^{2-} invasion into the concrete, which could result in micro structural damage and hydration product damage (Gu et al., 2019a). The salt crystallization corrosion is mainly represented by the gypsum crystal expansion and the mirabilite crystal separating-out, which produce crystal pressure inside the concrete (Feng et al., 2014). Many researchers have found that adding mineral admixture could help to improve the concrete performance in resisting sulfate corrosion (Huang et al., 2017; Nosouhian et al., 2019; Zhang et al., 2021b). Alapour et al. (Alapour and Hooton, 2017) determined from their study that, the application of certain amount of slag can delay the concrete deterioration caused by sulfate. Nabil M(Al-Akhras, 2006) believed that, replacing cement with 0–15% metakaolin can significantly enhance the concrete performance in resisting sulfate corrosion. However, in practical engineering, the concrete is usually subjected to corrosion brought by multiple types of ions, especially SO_4^{2-}, Mg^{2+}, and Cl^-. These three types of ions, which are widely distributed in saline soil and ocean, have the most serious adverse impact on concrete (Gu et al., 2019b). For the studies on metakaolin concrete when suffering corrosion brought by multiple types of ions, the test of Mardani (Mardani-Aghabaglou et al., 2014) showed that, facing the joint corrosion of Mg^{2+} and SO_4^{2-}, the adding of metakaolin would ease the damage brought by concrete expansion, but Lee et al. (2005) expressed the contrary opinion, believing that the adding of metakaolin could worsen the concrete damage when facing the joint corrosion of Mg^{2+} and SO_4^{2-}.

The aforementioned studies demonstrate the advantages of mineral admixtures. However, most of these studies focus on the concrete corrosion caused by a single type of corrosive ion, lacking studies on metakaolin concrete corrosion caused by multiple types of ions. And even the existing researches obtained contradictory conclusions. As a matter of fact, the concrete could be affected by the coupling effects of dry-wet alternation and corrosive ion corrosion, such as the large temperature difference and large water evaporation phenomenon in salt lake areas of West China region, and the alternated flood and tide ebb tides in coastal environment regions. The dry-wet alternation can increase the concrete porosity and accelerate the corrosive ion filtration (Qi et al., 2017), but its physical corrosion effect is usually ignored. Moreover there are also problems to be solved, for example: do various metakaolin contents have different impacts on corrosion brought by multiple types of corrosive ions? Will different corrosion time result in different results?

To solve the above problems, the dry-wet alternation test was carried out, in which, the 5%$MgSO_4$+3.5%NaCl solution was taken as the corrosion medium, the concretes were added with 5, 10, and 15% metakaolin respectively, and the ordinary concrete was taken as the control group, in order to study the influences of different metakaolin contents on the concrete performance in resisting corrosion brought by multiple types of corrosive ions. The compressive strength and mass of the concrete were measured for each cycle. And the comparison on differences among all groups of concretes was made as well. A series of micro analysis approaches, including the X-ray diffraction (XRD), Fourier transform infrared spectrum (FTIR), scanning electron microscope (SEM), and energy dispersive spectrum (EDS), were applied to explore the degradation mechanism of concretes with different metakaolin contents at the time of being eroded by multiple ions.

TEST PROCESS

Raw Material of Test

According to the industrial standards and the references of relevant literature (Peng et al., 2019; Zhou et al., 2021), the P.O. 42.5 ordinary Portland cement produced in Huainan City, and the white-color metakaolin with about 1.8 μm average particle size produced by Shanghai Lingdong Company were applied in this test. The chemical compositions of the metakaolin and the cement are as shown in **Table 1**. And for the aggregates, the gravels with 5–15 mm continuous gradation were used as the coarse aggregates, which are featured in 1,543 kg/m³ bulk density and 2,630 kg/m³ apparent density; and the medium sands coming from Huaihe River were used as the fine aggregates, which are with about 2.9 fineness modulus, 1,577 kg/m³ bulk density, and 2,621 kg/m³ apparent density. And the Polycarboxylate-based superplasticizer with about 37% water reduction rate was used as the water reducer in this test.

Mix Proportion and Preparation of Test Samples

Relative materials show (Abdul Razak and Wong, 2005; Pouhet and Cyr, 2016) that, the maximum content of metakaolin added into concrete shall be no more than 20%; and on the other hand, adding 5–15% metakaolin into the concrete could effectively improve the mechanical properties of the concrete. Therefore, the concrete proportioning was finally determined according to the JGJ55-2011 *Specification for mix proportion design of ordinary concrete* (as shown in **Table 2**). In this test, the metakaolin was

TABLE 1 | Cement and metakaolin chemical composition (%).

Composition	CaO	SiO_2	Al_2O_3	Fe_2O_3	SO_3	K_2O	P_2O_5	MgO	Na_2O	Loss
Cement	68.66	21.93	3.72	2.57	1.09	0.67	0.33	0.07	0.12	0.84
Metakaolin	0.04	57.03	41.06	0.71	0.13	0.16	0.11	0.08	0.11	0.57

TABLE 2 | Mix proportion of concrete (kg/m³).

Number	Sand	Aggregate	Cement	Metakaolin	Water	Water reducing agent
MK0	619	1,101	500	0	180	3
MK5	619	1,101	475	25	180	3.5
MK10	619	1,101	450	50	180	4
MK15	619	1,101	425	75	180	4.5

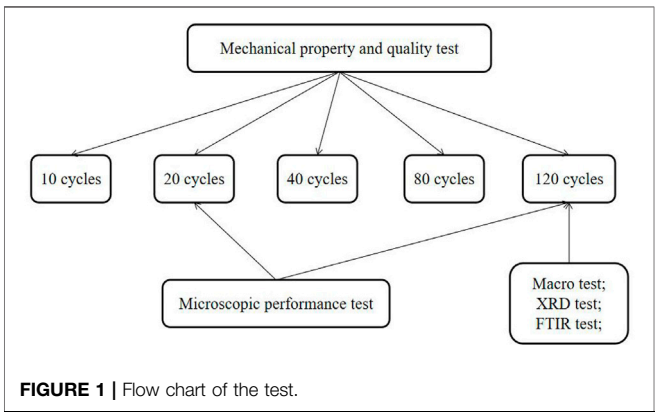

FIGURE 1 | Flow chart of the test.

used to equivalently replace 5, 10, and 15% Portland cements, based on which, the corresponding test samples were numbered as MK5, MK10, and MK15. Besides, the reference concrete was numbered as MK0 and taken as the control group. The concrete samples made for this test were non-standard blocks sized 100 × 100 × 100 mm. The process to make the concrete test samples is below: weigh and mix the sand and stone, and put the mixture into the mixer to mix for about 1 min, then weigh and mix the metakaolin and cement according to the ratio as shown in **Table 2** and mix for 2 mins until the cementing material and the aggregates are evenly mixed; finally, mix the water reducer with the clean water, and put the mixture into the mixer to mix with other materials evenly; after finishing the mixing, put the mixture into molds, and then move the molds to the vibration table to vibrate and compact; then put the molds aside and wait for 24 h; after that, demold and put the concrete samples in the standard curing room with (20 ± 2)°C temperature and over 95% humidity for 28 days before carrying out dry-wet alternation test.

Test Method

To simulate the physical and chemical corrosion in certain salt lake areas and coastal areas, the 5%$MgSO_4$+3.5%NaCl solution was taken as the corrosion medium, and the dry-wet alternation steps were determined according to the *Standard for test methods of long-term performance and durability of ordinary concrete* (GB/T50082-2009) (GB/T 50082-2009, 2009), the previous testing experience (Chen et al., 2021b), and the literature (Liu et al., 2020; Sun et al., 2021) for the test. The dry-wet alternation steps include: soak the test samples in the solution for 14 h → dry them in room temperature for 1 h → dry them in 60°C dryer for 8 h → cool them at room temperature for 1 h, totaling to 24 h per cycle. In order to maintain stable concentrations of all the solutions, we made new solutions and replaced every 10 days during the test. When the required cycles were reached, the tests on mechanical properties, mass, XRD, FTIR, macro, and micro performances were carried out on the test samples respectively. For specific flowchart of the test, please refer to **Figure 1**. Since the key study objects of this paper are the concretes that are added with different volumes of metakaolin, in order to show the differences among various groups of concrete samples obviously, the macro test, XRD test, and FTIR test were carried out when reaching the most representative "120 cycles".

When 10, 20, 40, 80, and 120 cycles were reached, the compressive strength and the mass of various groups of metakaolin concrete were tested. And the compressive-strength operation was performed according to GB/T50081-2002 specifications (GB/T 50081-2002, 2002). Since the test samples adopted in this test are non-standard blocks sized 100 × 100 × 100 mm, the coefficient of 0.95 was multiplied. Meanwhile the relative compressive strength was calculated according to **Eq. 1**. And the mass was measured by electronic balance (accurate to 0.01). Each test sample was weighed for three times, based on which, the average value was taken finally. And the rate-of-change of the mass was calculated by **Eq. 2**.

$$F_\alpha = 100\% \times \frac{F_N}{F_0} \tag{1}$$

Where F_α is the relative compressive strength, F_N is the compressive strength of concrete after N times of dry-wet alternation, F_0 is the MK concrete compressive strength that hasn't been eroded.

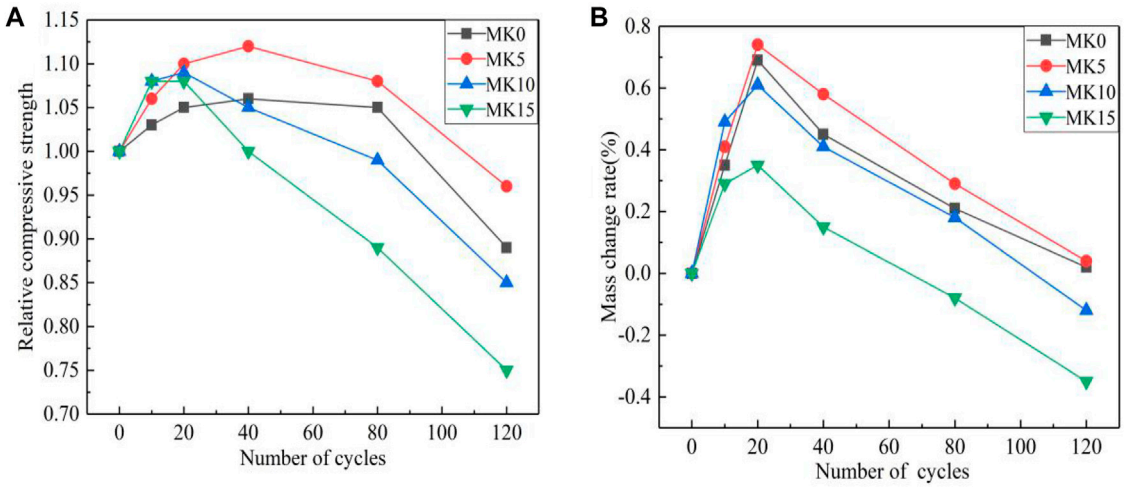

FIGURE 2 | Changes in physical properties of concrete: **(A)** Relative compressive strength; **(B)** Mass change rate.

$$\Delta M = 100\% \times \frac{M_N - M_0}{M_0} \quad (2)$$

Where ΔM is the mass change rate of the test sample, M_N is the test sample mass after N times of dry-wet alternations, and M_0 is the test sample mass before corrosion.

When reaching 120 cycles, XRD and FTIR tests were carried out on the concretes with different metakaolin contents in order to analyze the phase composition of the corrosion products. The D/max-2550 XRD machine with 5°~95°scanning range produced by Japan was used in this test. And the scanning step was set as 0.02 in the test; the NICOLET IS 50 infrared spectrometer with 350 cm^{-1}~7800 cm^{-1} wave number range produced by the USA was used for the FTIR test in this study.

When 20 and 120 cycles were reached, Hitachi S4800 cold field SEM produced by Japan and EDS machine were used to observe and analyze the micro morphology of each sample. The accelerating voltage is 5 KV. Adjust the magnification to 10,000 times when observing the samples with 20 cycles. For the samples with 120 cycles, set the magnification to 20,000 times or 50,000 times for observation. Before SEM observation, the mortar slices with 2–4 mm thickness were taken from the surface of the test samples and put into absolute ethyl alcohol to terminate hydration. After that, the slices were put into dryer with 60 ± 5°C temperature till reaching constant mass. The test samples were carried out with grinding and polishing treatment, as well as vacuuming and conductive coating treatment to improve the conductivity. Finally, the SEM test was carried out.

RESULTS

Changes of Physical Properties

Figure 2 shows the physical property changes of concretes added with 5, 10, and 15% metakaolin respectively. In general, the trend of relative compressive strength changes of the concrete added with metakaolin is: rising stage →flat stage→declining stage→rapid declining stage. And the trend of the mass changes is: rising stage →flat stage→declining stage.

For the corrosion time impact on concrete performance, at the initial stage (about 0–20 cycles), the corrosion products, such as ettringite and magnesium hydroxide, were produced firstly, which filled up the internal pores inside the concrete to some certain extent. This promoted the rising of the compressive strength and the mass of the concrete. Meanwhile due to the pozzolanic activity of the metakaolin, lots of hydration products were produced inside the concretes, so that the mass of the test samples increased slightly. However with the continuous increase of dry-wet alternation times, the corrosion products kept accumulating in quantity and volume, which resulted in cracking and mortar aggregates peeling-off on concrete surface. In this case, the compressive strength and the mass kept declining during this period.

For impacts of metakaolin contents on concrete performance, during 0–10 cycles, with the increase of metakaolin contents, the compressive strength improved gradually due to two reasons: first, the concrete during 0–10 cycles was still at hydration stage, and the large amount of Al_2O_3 contained in the metakaolin accelerated the hydration process (Coleman and Mcwhinnie, 2000); second, the small diameter of the metakaolin filled up the pores inside the cement, which resulted in particle gradation and improved the concrete compactness. However the metakaolin increase also brought with adverse effects. When the metakaolin content reached 10%, the relative compressive strength increased by 1.08% during the process of 0–10 cycles. But when the metakaolin content reached 15%, the increase of relative compressive strength still remained at 1.08%. That's because the metakaolin has large specific surface area, and its particles are in flake shape. Excessive content of metakaolin would induce agglomeration. Therefore, too much metakaolin is non-conductive to the concrete performance development (Vance et al., 2013). With the increase of cycles, the physical

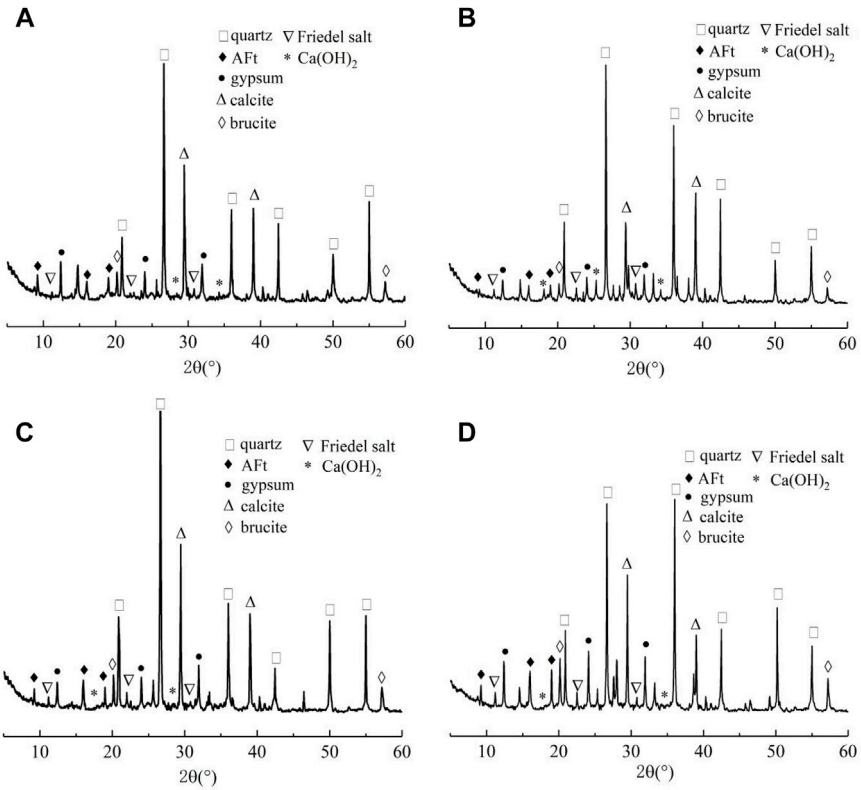

FIGURE 3 | XRD pattern of specimen when erosion days are 120 days: **(A)** MK0; **(B)** MK5; **(C)** MK10; **(D)** MK15.

property of each group of concrete samples are: MK5 > MK0 > MK10 > MK15. The metakaolin contains a great number of SiO_2, so it can promote the massive M-S-H generating. And the forming of M-S-H can soften the cement, inducing serious declining of the physical properties of the concrete. When reaching 120 cycles, the relative compressive strength of MK10 was only 0.85 while the mass changing rate was −0.12%. And the same two data of MK15 were 0.75% and −0.35% respectively. Compared with MK10 and MK15, MK5 physical properties always ranked at high position, reaching 0.96% relative compressive strength and 0.04% mass changing rate after 120 cycles. That's mainly because the metakaolin makes MK5 compact during the concrete hydration process, and the relatively small metakaolin content prevents massive generating of M-S-H, which reduces the chemical corrosion brought to the concrete.

Phase Composition Analysis

X-Ray Diffraction Analysis

The X-ray diffraction was applied to analyze the corrosion products, in order to further study the concrete degradation mechanism under corrosion of multiple types of ions, and study the influences of metakaolin content changes on the concrete phase composition.

Figure 3 shows the XRD maps of concrete with different metakaolin contents. With the changes of metakaolin contents, the phase compositions vary, which is mainly manifested in the disappearing and occurrence of diffraction peaks and the intensity changes. The two highest diffraction peaks in the figure are quartz and calcite, which are both from the aggregates of the concrete. Besides, it can be seen that the diffraction peaks of $Ca(OH)_2$ and Friedel salt of the four types of concretes are quite weak. That's because at the later stage of corrosion, the Mg^{2+} and SO_4^{2-} enter inside the concrete, consuming great number of $Ca(OH)_2$ and generating corrosion products of ettringite, gypsum, and magnesium hydroxide. This leads to sharp drop of pH value inside the test samples. Meanwhile, Friedel salt can decompose gradually in low-pH environment (Cheng et al., 2019). By making comparison on the four groups of concretes, it can be found that the diffraction peaks of $Ca(OH)_2$ and Friedel salt of MK5 were higher than those of MK0, MK10, and MK15, and on the other hand, the diffraction peaks of the its corrosion products, such as the ettringite, gypsum, and magnesium hydroxide, were lower than those of other groups. Based on the above, it can be deduced that, MK5 has better performance in resisting compound salts corrosion than the other two groups at this time. That is because in the early stage of corrosion, the concrete compactness is high due to the effect of metakaolin, and the corrosive ion diffusion speed is slowed down. After that, with the increase of corrosion time, it generated limited volume of M-S-H inside MK5 concrete, and the undecalcified C-S-H physically absorbed SO_4^{2-} and Cl^- (Yuan et al., 2009) to some extent, which reduced the generating of corrosion products, and improved the

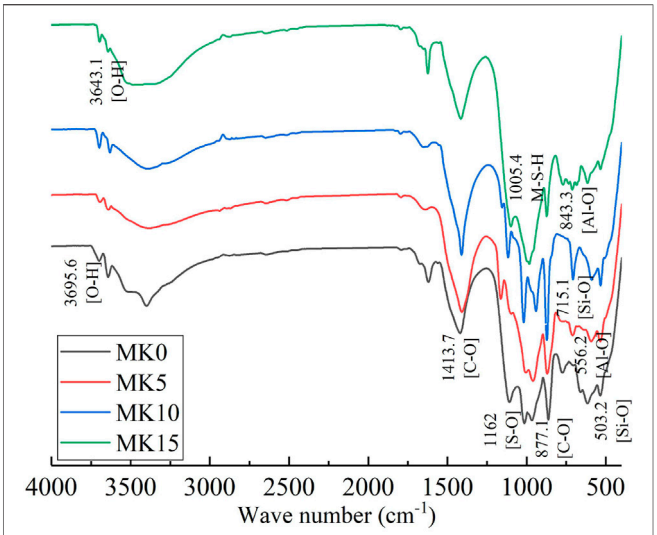

FIGURE 4 | FTIR diagram of concrete with different metakaolin content.

concrete durability. For MK0, MK10, and MK15, since these groups of samples had weaker performance in resisting corrosion and low pH than those of MK5 at this time, they experienced ettringite decomposition and weakened generating of secondary ettringite, but accelerated generating of gypsum. Besides, Mg^{2+} diffused faster in low pH environment (De Weerdt et al., 2019), which greatly increased the contents of M-S-H and magnesium hydroxide. And since the metakaolin contained massive active SiO_2, the increase of metakaolin content accelerated the generating of M-S-H, and resulted in worse damage to the concrete. Therefore the diffraction peaks of ettringite, gypsum, and magnesium hydroxide of MK10 are higher than those of MK5 and MK0. And the diffraction peaks of corrosion products in MK15 reach the maximum.

Fourier Transform Infrared Spectrum Analysis

It is hard to use X-ray diffraction to identify ettringite and thaumasite. Therefore the FTIR spectrum was applied for testing in this study, which can not only identify the ettringite and thaumasite, but also prove the existence of M-S-H.

Figure 4 shows the infrared spectrogram of the concretes with different metakaolin contents. It can be seen that stretching vibration peak of S-O(SO_4^{2-}) exist at 1,162 cm^{-1}. Besides, bending vibration peaks corresponding to Al-O bond also exist at wave numbers of 843.3 and 556.2 cm^{-1}. That's the evidence proving the existence of ettringite. The strong peaks at 877.1 and 1,413.7 cm^{-1} are induced by the bending and stretching vibrations of C-O bond (CO_3^{2-}). This indicates the existence of massive calcite (Wang et al., 2019) coming from the concrete aggregates. The silicon in the thaumasite and the hydroxyl combined in hexacoordinated form, generating the octahedron group. In this figure, the bending vibration peak of Si-O bond (SiO_6) appears at 503.2 cm^{-1}. And the stretching vibration peak corresponding to Si-O bond exists at 715.1 cm^{-1}. This indicates the existence of thaumasite in corrosion products (Deng et al., 2005).

It can be known from relative articles (Bernard et al., 2017) that, the characteristic peak of M-S-H in the figure appears at 1005.4 cm^{-1}. It can be seen that comparatively weak shoulder peaks of MK0 and MK5 appear at this position with similar peak sizes. This further indicates that, a few content of metakaolin added in concrete won't produce excessive M-S-H. MK10 shows comparatively sharp characteristic absorption peak here, indicating the enlargement of peak value at this position. The characteristic absorption peak of MK15 gets broader and the peak value increase further. Besides, compared to samples MK0 and MK5, peaks of MK10 and MK15 at 556.2 cm^{-1} become stronger with the increase of metakaolin contents. This shows that the ettringite content also increases gradually. Therefore the ettringite contents of MK15 and MK10 are higher than those of MK0 and MK5. This confirms to the conclusions obtained by XRD test. The characteristic absorption peak of O-H is at 3643.1 cm^{-1}, which is with small peak value. It means that the test samples contain $Ca(OH)_2$ (Song et al., 20142014) at this time, which is in extremely small amount. Through the XRD test and FTIR test, it can be known that the complex salt corrosion to the concrete produces complicated corrosion products. The generating of ettringite, gypsum, Friedel salt, magnesium hydroxide, M-S-H, and thaumasite consumes great number of $Ca(OH)_2$.

Macro Analysis

Figure 5 shows the macro-morphology images of the four types of concretes with different metakaolin contents that are subjected to corrosion of multiple types of ions after 120 cycles. Generally, three types of corrosive ions of Mg^{2+}, SO_4^{2-}, and Cl^- mainly cause peeling-off of surface aggregates, and cracking and peeling-off of corners. With the increase of metakaolin contents, the peeling-off of the surface mortar and aggregates seems more obvious.

MK0 is the ordinary concrete. It can be seen that significant deterioration appears on its edges. The edges are damaged and have small crack development. Holes can be seen on the bottom of the test samples. But the mortar particles peeling-off seems not serious on the surface of the concrete.

MK5 is the concrete with 5% metakaolin. Compared with MK0, MK5 is featured in better concrete integrity and less peeling-off of edges and corners, but significant surface aggregate peeling-off. Powders and slightly exposed coarse aggregates can be seen on the concrete surface. When the metakaolin content increases to 10%, large areas of aggregates peel off from the surface of MK10 concrete. Its exposed amount of coarse aggregates is significantly greater than that of the MK5, and is accompanied with big holes. When the metakaolin content reaches 15%, the damage to the concrete further gets worse. Compared with MK10, the surface mortar structure of MK 15 has been totally damaged by M-S-H. Edges of the test sample peel off. The concrete, as a whole, suffers serious damage.

Due to the high pozzolanic activity, the metakaolin could produce massive C-S-H in alkali environment. The two ions of calcium and magnesium are with similar radius of 4.1 and 4.3 radius respectively. So when the concrete is eroded by Mg^{2+}, the C-S-H could be easily decalcified and decomposed, forming non-cementing M-S-H. Besides, the active SiO_2 in metakaolin would

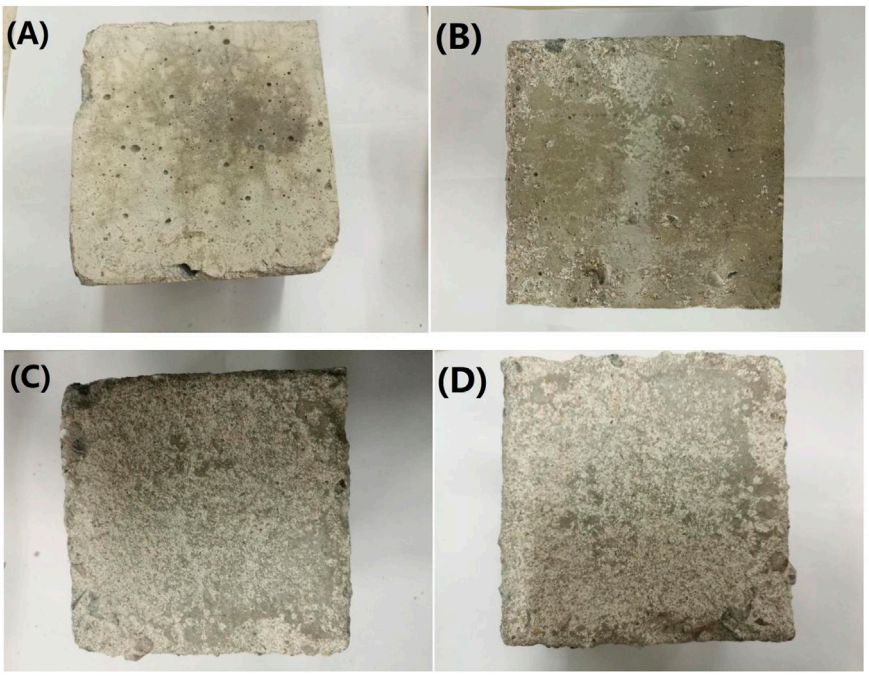

FIGURE 5 | Macro-morphology characteristics of the specimen when it is corroded by corrosive ions:**(A)** MK0; **(B)** MK5;**(C)** MK10; **(D)** MK15.

also promote the generating of M-S-H. Therefore, excessive metakaolin content would result in massive generating of M-S-H, seriously reducing the concrete durability.

Micro Analysis

Figure 6 shows the micro-morphology of the four groups of contents with different metakaolin contents after 20 cycles of corrosive ion corrosion. It can be seen that, at the initial stage of corrosion, thereare little corrosion products but many hydration products. The increase of metakaolin contents has a great impact on the micro-structure compactness and the pore characteristics of the concrete.

From **Figure 6**, it can be seen that, the MK0 micro-structure is compacted at this time. Besides the pores with different sizes on the surface, lots of needle-shaped ettringite inserted inside the pores can also be seen in this figure. Compared with MK0, the micro-structure of MK5 is more compacted. Though it has a small number of ettringite, the pores amount is comparatively reduced. Meanwhile at this time, most of the unhydrated particles and hydration products are closely connected. When the metakaolin content reaches 10%, the concrete surface is covered by massive C-S-H cementing materials in screen-shaped structure. Due to the high pozzolanic activity of the metakaolin, the cement and the metakaolin particles are covered by numerous hydration products, which further improves the compactness. However excessive metakaolin content would also result in agglomeration, reducing the concrete performance (Vance et al., 2013). That is also the reason causing the bad micro-structure connection, massive exposure of cement and metakaolin particles, and more significant pores and cracks of MK15 than the situations of MK10. Combining with the physical properties shown in **Figure 2**, it can be known that, concrete with proper metakaolin content has excellent durability at the early corrosion stage; when the metakaolin content reaches 10%, the concrete shows high compactness and most capable durability.

However when the corrosion time reaches 120 cycles, the micro-morphology of the four types of contents with different metakaolin contents are as shown in **Figure 7.** The EDS analysis was carried out in order to figure out the corrosion products, please see **Figure 8.**

When the corrosion reaches 120 cycles, the MK0 shows massive pores and very bad overall integrity. A small part of screen-shaped materials attach on its surface. The EDS analysis indicates that, the material was mainly composed of O,Ca,Si, and S. Therefore it can be inferred that the material is the hydration product C-S-H. At this time, there's only a little C-S-H, most of which have been converted into M-S-H. For MK5, it can be seen that many needle-shaped materials fill up the micro structure. And the EDS analysis results, as shown in **Figure 8B**, indicate that the material is mainly composed of Ca,S,Al, and O. According to the morphology features of this material (Sarkar et al., 2010; Nehdi et al., 2014), it can be inferred that the material is ettringite. These needle-shaped ettringite distribute randomly without any order, and are surrounded by a few pores and cracks. For MK10 with 10% metakaolin content, besides the needle-shaped ettringite, it also shows many plate-shaped corrosion products, which are proved to be composed of Ca,S, and O by EDS analysis. According to relative literature (Tan et al., 2017), it can be roughly judged that the material is gypsum. And at this time, the gypsum

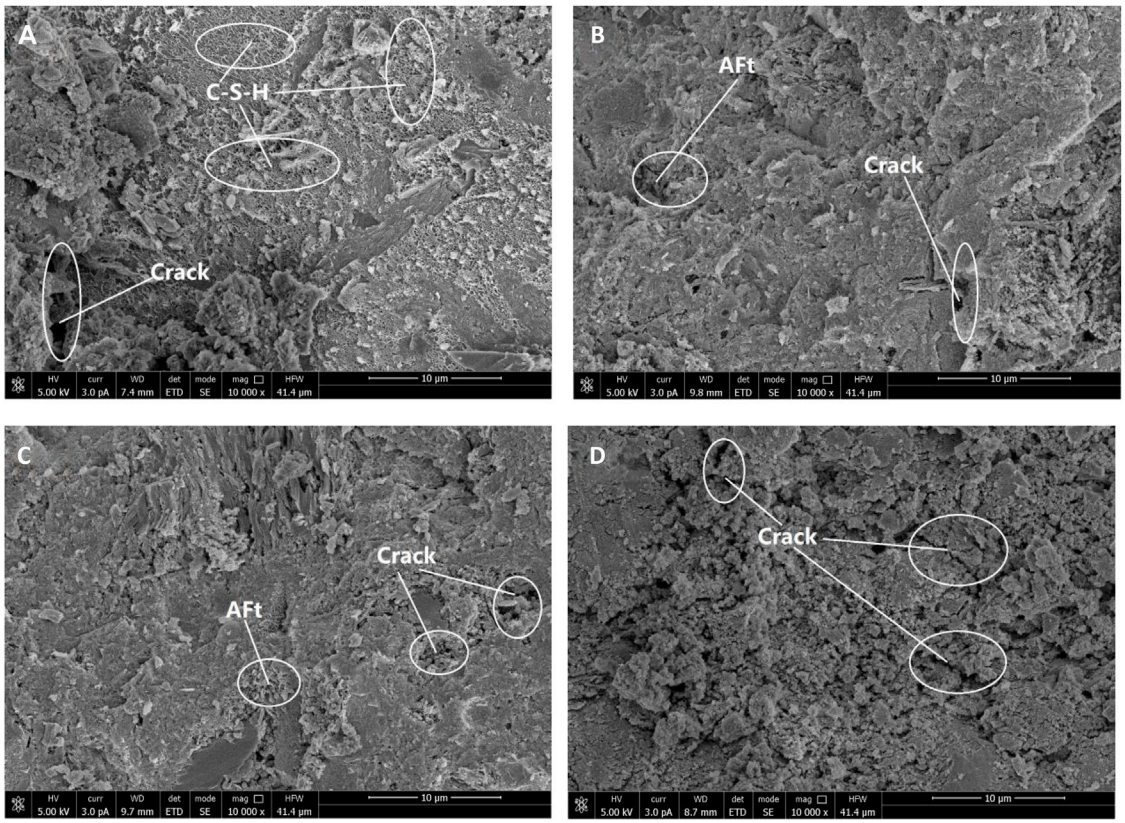

FIGURE 6 | Microscopic morphology of each group of concrete with 20 cycles: **(A)** MK0; **(B)** MK5; **(C)** MK10; **(D)** MK15.

crystal has developed abnormally large and overlapped. They interact and exist in the pores of the concrete, with part of the crystals covered by the surrounded M-S-H. Since MK10 contains more metakaolin, with the increase of corrosion time, the M-S-H content gradually increases, which leads to the increase of aggregate peeling-off and pores on the concrete surface. This not only provides channels to the SO_4^{2-} invasion, but also the space for corrosion product stacking. The SO_4^{2-} invasion again brings the test samples with secondary corrosion damage. When the metakaolin content reaches 15%, the concrete shows very bad internal connection of its micro structure, significantly increased pores with large sizes, and loose and porous characteristics. Besides, massive needle-shaped ettringite can also be seen. Compared with the ettringite shape of MK5, the ettringite of MK15 is thin and compact, which might be the secondary ettringite caused by the secondary M-S-H damage to the test samples. Meanwhile a certain amount of flocculent material is found around the pores, please refer to EDS of **Figure 8D**. This material is mainly composed of Mg,Si,O, and S. According to the micro morphology features (Li et al., 2014), it can be judged that the material might be M-S-H. Combining with the macro-morphology figure, when the operation reached 120 cycles, the concrete turns to have increased internal pores and cracks (**Figure 7**) due to the joint effects of expansion stress of corrosion products, pressure of salt crystals, and surface tension formed by the solution in the capillary pores during the dry-wet alternation process. The increased internal pores and cracks connect with the surface cracks, which result in the peeling-off of concrete edges and corners (**Figure 5**), thereby causing rapid reduction of concrete mass and compressive strength.

The results of 120 cycles are quite different from the those of 20 cycles. This is the later stage of corrosion. According to the XRD analysis and the FTIR analysis, the MK10 and MK15 are featured in loose and porous micro structure due to the M-S-H impact at this time. But MK5 still has closely connected hydration products, comparative compact micro structure, relatively small amount of corrosion products (**Figures 3**, **4**), and optimal durability.

DISCUSSIONS

Impacts of Single SO_4^{2-} on Metakaolin Concrete

There are many studies carried out on single SO_4^{2-} impacts on metakaolin concrete. NaBil M added 0~15% metakaolin in the concrete. With the increase of metakaolin content, the concrete performance in resisting sulfate salt corrosion enhances accordingly (Al-Akhras, 2006). The sulfate salt corrosion to the metakaolin concrete mainly produces ettringite, gypsum, and mirabilite crystal (Hu and He, 2020). During the SO_4^{2-}

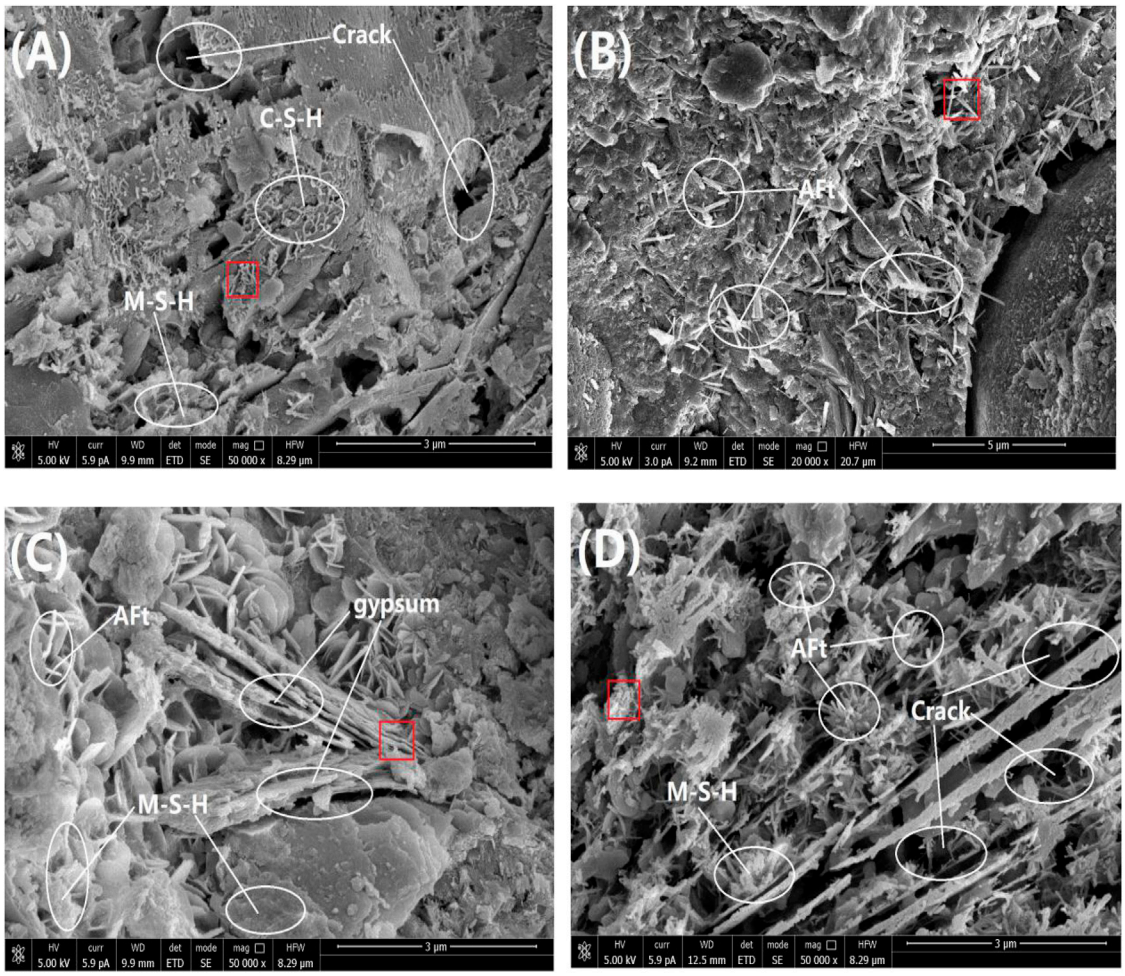

FIGURE 7 | Microscopic morphology of each group of concrete with 120 cycles: **(A)** MK0; **(B)** MK5; **(C)** MK10; **(D)** MK15.

corrosion to the concrete, the tricalcium aluminate and $Ca(OH)_2$ react with SO_4^{2-} and produce excessive ettringite and gypsum, which can seriously damage the concrete performance. The reason why the metakaolin is conductive in improving concrete's resistance to sulfate salt (Zheng et al., 2021) can be concluded into two points: first, the replacement of part of cement by metakaolin reduces the tricalcium aluminate content in the cement accordingly, thereby reducing the generated volume of corrosion products; second, due to the high pozzolanic activity, the metakaolin could react with $Ca(OH)_2$ inside the concrete, and produce massive C-S-H and C-A-S-H, which narrow the pores inside the concrete and enhance the compactness of the concrete.

The key point of this paper is the impact of compound salts on metakaolin concrete. Being different from the single SO_4^{2-} corrosion, with the increase of metakaolin content, the concrete's resistance to compound salts corrosion increases first, and then reduces. The main reason explaining this phenomenon is the M-S-H impact. Single SO_4^{2-} corrosion to metakaolin concrete only produces ettringite and gypsum. But the compound salts corrosion could produce complicated corrosion products, which includes M-S-H, magnesium hydroxide, thaumasite, and Friedel salt besides the ettringite and gypsum. Therefore under the joint effects of the corrosion products, the metakaolin concrete performance drops rapidly.

Joint Effects of Corrosive Ions

The mechanism of corrosive ions of SO_4^{2-},Mg^{2+}, and Cl^- on the concrete is complicated. The corrosion of multiple types of ions usually exist at the same time, and could promote or inhibit the corrosion effect of each other.

For Cl^-, it has little corrosive effect inside the concrete, instead, it mainly erodes the rebars. However the chloride salt could affect the corrosion of O_4^{2-} and Mg^{2+} to some certain extent during the corrosion process. At the early stage of corrosion, since Cl^- could diffuse rapidly due to its small volume, it could combine with Al prior to SO_4^{2-}, and generate Friedel salt (as shown in **Eq. 3**), thereby preventing the generating of ettringite (Deng et al., 2005). In this case, it can be said that Cl^- and $SO_4^{2-}$are mutually inhibited. But at the latter stage of the corrosion, with the reduction of the hydration products inside the test samples, the pH value of the corrosive layer of concrete reduces. As a

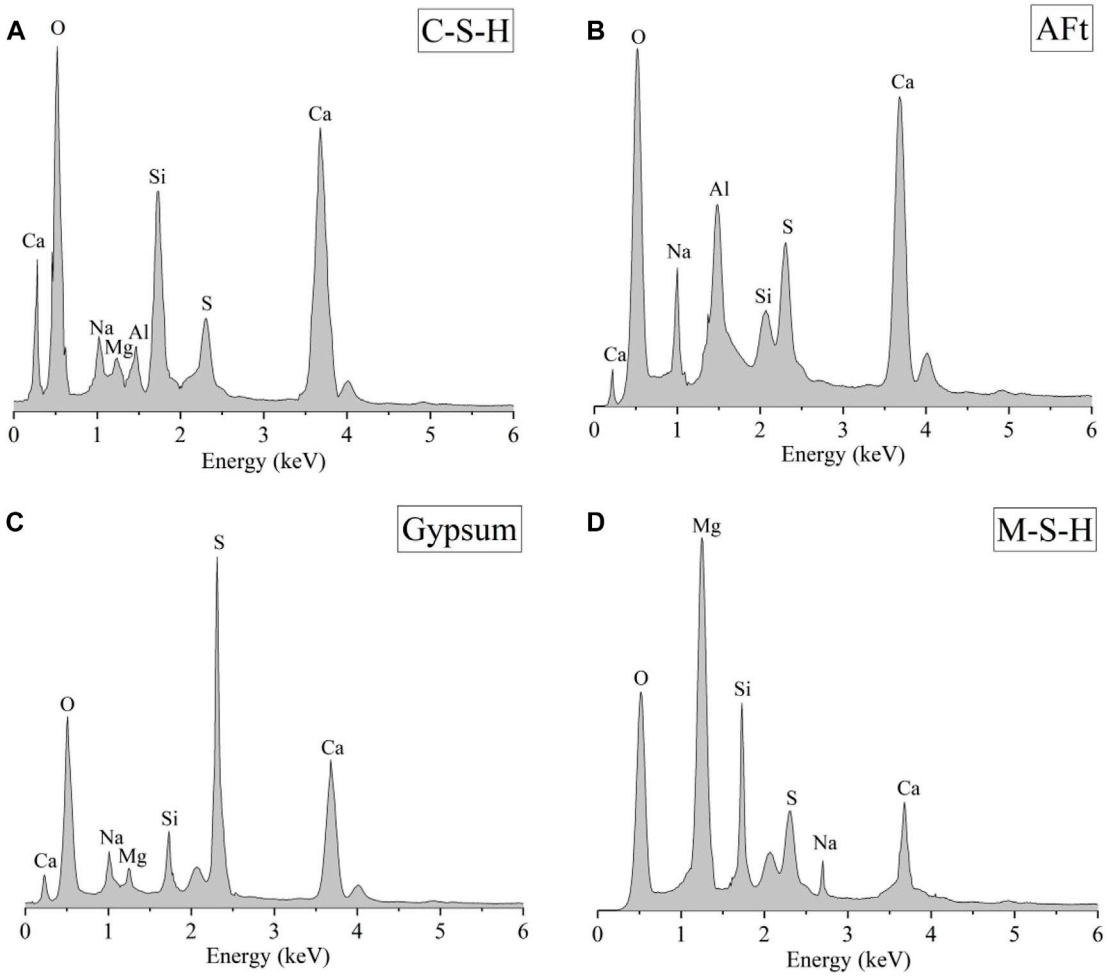

FIGURE 8 | EDS spectrum when the number of cycles is 120:**(A)** C-S-H; **(B)** AFt; **(C)** Gypsum; **(D)** M-S-H.

matter of fact, Friedel salt is unstable in low pH environment, and could hydrolyze (as shown in **Eq. 4**) to release massive free Cl^- inside the concrete. These free Cl^- could diffuse to deeper position of the test samples (Cheng et al., 2019).

Mg^{2+} is one of the main reasons causing pH value reduction, because Mg^{2+} could combine with $Ca(OH)_2$ inside the concrete to generate magnesium hydroxide with very-low solubility (**Eq. 5**). This could damage the alkali environment. Meanwhile, Ca^{2+} inside the hydration product C-S-H decalcifies and forms non-cementing M-S-H (**Eq. 6**), which could result in aggregate peeling-off from the surface of the concrete.

Iron synergy has great impact on concrete. With the increase of corrosion time, the pH value inside the test sample decreases further, Mg^{2+} diffusion accelerates, and the Friedel salt decomposes and generate a great number of Cl^- inside the concrete. Meanwhile the accelerating of Mg^{2+} invasion results in more generated M-S-H inside the concrete, which leads to the aggregate peeling-off, and the increase of internal cracks and pores of the test samples. This promotes the secondary invasion of SO_4^{2-} into the concrete, which produces more ettringite and gypsum, and results in secondary expansion damage to the concrete.

$$2Cl^- + Ca_3Al_2O_6 + Ca(OH)_2 + 10H_2O \rightarrow Ca_3Al_2O_6 \cdot CaCl_2 \cdot 10H_2O + 2OH^- \quad (3)$$

$$Ca_3Al_2O_6 \cdot CaCl_2 \cdot 10H_2O \rightarrow 2Al(OH)_4^- + 4Ca^{2+} + 2Cl^- + 4OH^- + 2H_2O \quad (4)$$

$$Mg^{2+} + Ca(OH)_2 \rightarrow Ca^{2+} + Mg(OH)_2 \quad (5)$$

$$3Mg^{2+} + 3CaO \cdot 2SiO_2 \cdot 3H_2O \rightarrow 3Ca^{2+} + 3MgO \cdot 2SiO_2 \cdot 3H_2O \quad (6)$$

CONCLUSION

In this paper, the impacts of different metakaolin contents on concrete durability under dry-wet alternation and joint corrosion of multiple types of ions were systematically analyzed. According to the results, conclusions as follows are obtained:

1) Under the corrosion of multiple types of corrosive ions, with the increase of the corrosion time, the physical properties of the test samples show tendency of rising first and then declining. At the early stage of corrosion (20 cycles), the concrete with 10% metakaolin content has the optimal physical properties. At the latter stage of the corrosion (120 cycles), concrete with 5% metakaolin content shows the optimal physical properties.
2) Main corrosion products generated by the joint corrosion of multiple types of corrosive ions on concrete under dry-wet alternation are: ettringite, gypsum, Friedel salt, magnesium hydroxide, M-S-H, and thaumasite. The corrosion product quantity of the concrete with 5% metakaolin is similar to that of the ornidary concrete. But with the increase of metakaolin, the quantity of corrosion products increase, especially the M-S-H shows the most significant increase in quantity.
3) When suffering joint corrosion of multiple types of corrosive ions, the metakaolin concrete, from the macro aspect, shows aggregate peeling-off and crack generating. The test sample represents powder-state surface. The increase of added metakaolin results in the increase of the surface aggregate peeling-off.
4) 10% metakaolin makes the micro structure of the concrete more compact at the early stage; then at the later stage, 5% metakaolin can improve the connection of the internal micro structure of the test sample, reducing pores. Since Mg^{2+} has very great impact on metakaolin concrete, excessive metakaolin leads to significant reduction of concrete durability, and loose and porous micro morphology.

DATA AVAILABILITY STATEMENT

The original contributions presented in the study are included in the article/supplementary material, further inquiries can be directed to the corresponding author.

AUTHOR CONTRIBUTIONS

CX wrote most of this manuscript. CX was in charge of implementing most of the materials manufacturing and properties testing. PJ and SZ are responsible for providing funds and checking manuscripts. All authors have read and agreed to the published version of the manuscript.

FUNDING

This research was funded by the Key Projects of Natural Science Research in Colleges and universities of AnhuiProvince, Grantnumber KJ2019A1043; Science and Technology Project of Jiangsu Provincial Department of Housing and Urban Rural Development, Grant number 2019ZD001190.

REFERENCES

Abdul Razak, H., and Wong, H. S. (2005). Strength Estimation Model for High-Strength concrete Incorporating Metakaolin and Silica Fume. *Cem. Concr. Res.* 35, 688–695. doi:10.1016/j.cemconres.2004.05.040

Al-Akhras, N. M. (2006). Durability of Metakaolin concrete to Sulfate Attack. *Cem. Concr. Res.* 36, 1727–1734. doi:10.1016/j.cemconres.2006.03.026

Alapour, F., and Hooton, R. D. (2017). Sulfate Resistance of Portland and Slag Cement Concretes Exposed to Sodium Sulfate for 38 Years. *ACI Mater. J.* 114, 477–490. doi:10.14359/51689678

Andrew, R. M. (2019). Global CO2 Emissions from Cement Production,1928-2018. *Earth Syst. Sci. Data.* 4, 1675–1710. doi:10.5194/essd-11-1675-2019

Bernard, E., Lothenbach, B., Rentsch, D., Pochard, I., and Dauzères, A. (2017). Formation of Magnesium Silicate Hydrates (M-S-H). *Phys. Chem. Earth, Parts A/B/C* 99, 142–157. doi:10.1016/j.pce.2017.02.005

Bildirici, M. E. (2019). Cement Production, Environmental Pollution, and Economic Growth: Evidence from China and USA. *Clean. Techn Environ. Pol.* 21, 783–793. doi:10.1007/s10098-019-01667-3

Chen, X., SunPang, Z. J., and Pang, J. (2021). A Research on Durability Degradation of Mineral Admixture Concrete. *Materials* 14, 1752. doi:10.3390/ma14071752

Chen, X., Sun, Z., and Pang, J. (2021). Effects of Various Corrosive Ions on Metakaolin Concrete. *Crystals* 11, 1108. doi:10.3390/cryst11091108

Cheng, S., Shui, Z., Sun, T., Gao, X., and Guo, C. (2019). Effects of Sulfate and Magnesium Ion on the Chloride Transportation Behavior and Binding Capacity of Portland Cement Mortar. *Constr. Build. Mater.* 204, 265–275. doi:10.1016/j.conbuildmat.2019.01.132

Coleman, N. J., and Mcwhinnie, W. R. (2000). The Solid State Chemistry of Metakaolin-Blended Ordinary Portland Cement. *J. Mater. Sci.* 35, 2701–2710. doi:10.1023/a:1004753926277

De Weerdt, K., Lothenbach, B., and Geiker, M. R. (2019). Comparing Chloride Ingress from Seawater and NaCl Solution in Portland Cement Mortar. *Cem. Concr. Res.* 115, 80–89. doi:10.1016/j.cemconres.2018.09.014

Deng, D. H., Xiao, J., Yuan, Q., Zhang, W. N., and Liu, Y. X. (2005). On Thaumasite Incementitious Materials. *J. Build. Mater.* 8, 400–409.

Environment, U., Scrivener, K. L., John, V. M., and Gartner, E. (2018). Eco-efficient Cements: Potential Economically Viable Solutions for a low-CO2 Cement-Based Materials Industry. *Cem. Concr. Res.* 114, 2–26. doi:10.1016/j.cemconres.2018.03.015

Feng, P., Miao, C., and Bullard, J. W. (2014). A Model of Phase Stability, Microstructure and Properties during Leaching of Portland Cement Binders. *Cem. Concr. Compos.* 49, 9–19. doi:10.1016/j.cemconcomp.2014.01.006

GB/T 50081-2002 (2002). *Standard for Test Method of Mechanical Properties on Ordinary Concrete*. Beijing,China: China Building Industry Press.

GB/T 50082-2009 (2009). *Standard for Test Method of Long-Term Performance and Durability of Ordinary Concrete*. Beijing, China: Chinese Standard Institution Press.

Gu, Y., Martin, R.-P., Omikrine Metalssi, O., Fen-Chong, T., and Dangla, P. (2019). Pore Size Analyses of Cement Paste Exposed to External Sulfate Attack and Delayed Ettringite Formation. *Cement Concr. Res.* 123, 105766. doi:10.1016/j.cemconres.2019.05.011

Gu, Y., Martin, R.-P., Omikrine Metalssi, O., Fen-Chong, T., and Dangla, P. (2019). Pore Size Analyses of Cement Paste Exposed to External Sulfate Attack and Delayed Ettringite Formation. *Cem. Concr. Res.* 123, 105766. doi:10.1016/j.cemconres.2019.05.011

Hemalatha, T., and Ramaswamy, A. (2017). A Review on Fly Ash Characteristics - towards Promoting High Volume Utilization in Developing Sustainable concrete. *J. Clean. Prod.* 147, 546–559. doi:10.1016/j.jclepro.2017.01.114

Hu, L., and He, Z. (2020). A Fresh Perspective on Effect of Metakaolin and limestone Powder on Sulfate Resistance of Cement-Based Materials. *Constr. Build. Mater.* 262, 119847. doi:10.1016/j.conbuildmat.2020.119847

Huang, H., Gao, X., Wang, H., and Ye, H. (2017). Influence of rice Husk Ash on Strength and Permeability of Ultra-high Performance concrete. *Constr. Build. Mater.* 149, 621–628. doi:10.1016/j.conbuildmat.2017.05.155

Jiang, G., Rong, Z., and Sun, W. (2015). Effects of Metakaolin on Mechanical Properties, Pore Structure and Hydration Heat of Mortars at 0.17 W/b Ratio. *Constr. Build. Mater.* 93, 564–572. doi:10.1016/j.conbuildmat.2015.06.036

Jiang, Y. (2005). Study on Early Cracking Resistant Mechanical Characteristics of Fly-Ash Concrete. *Large Dam Saf.* 03, 34–37.

Juenger, M. C. G., and Siddique, R. (2015). Recent Advances in Understanding the Role of Supplementary Cementitious Materials in concrete. *Cem. Concr. Res.* 78, 71–80. doi:10.1016/j.cemconres.2015.03.018

Lee, S. T., Moon, H. Y., Hooton, R. D., and Kim, J. P. (2005). Effect of Solution Concentrations and Replacement Levels of Metakaolin on the Resistance of Mortars Exposed to Magnesium Sulfate Solutions. *Cem. Concr. Res.* 35, 1314–1323. doi:10.1016/j.cemconres.2004.10.035

Li, Z., Zhang, T., Hu, J., Tang, Y., Niu, Y., Wei, J., et al. (2014). Characterization of Reaction Products and Reaction Process of MgO-SiO2-H2o System at Room Temperature. *Constr. Build. Mater.* 61, 252–259. doi:10.1016/j.conbuildmat.2014.03.004

Liu, F., Zhang, T., Luo, T., Zhou, M., Zhang, K., and Ma, W. (2020). Study on the Deterioration of Concrete under Dry-Wet Cycle and Sulfate Attack. *Materials* 13, 4095. doi:10.3390/ma13184095

Mardani-Aghabaglou, A., İnan Sezer, G., and Ramyar, K. (2014). Comparison of Fly Ash, Silica Fume and Metakaolin from Mechanical Properties and Durability Performance of Mortar Mixtures View point. *Constr. Build. Mater.* 70, 17–25. doi:10.1016/j.conbuildmat.2014.07.089

Mo, Z., Wang, R., and Gao, X. (2020). Hydration and Mechanical Properties of UHPC Matrix Containing limestone and Different Levels of Metakaolin. *Constr. Build. Mater.* 256, 119454. doi:10.1016/j.conbuildmat.2020.119454

Nehdi, M. L., Suleiman, A. R., and Soliman, A. M. (2014). Investigation of concrete Exposed to Dual Sulfate Attack. *Cem. Concr. Res.* 64, 42–53. doi:10.1016/j.cemconres.2014.06.002

Nosouhian, F., Fincan, M., Shanahan, N., Stetsko, Y. P., Riding, K. A., and Zayed, A. (2019). Effects of Slag Characteristics on Sulfate Durability of Portland Cement-Slag Blended Systems. *Constr. Build. Mater.* 229, 116882. doi:10.1016/j.conbuildmat.2019.116882

Peng, H., Cui, C., Cai, C. S., Liu, Y., and Liu, Z. (2019). Microstructure and Microhardness Property of the Interface between a metakaolin/GGBFS-Based Geopolymer Paste and Granite Aggregate. *Constr. Build. Mater.* 221, 263–273. doi:10.1016/j.conbuildmat.2019.06.090

Pouhet, R., and Cyr, M. (2016). Formulation and Performance of Flash Metakaolin Geopolymer Concretes. *Constr. Build. Mater.* 120, 150–160. doi:10.1016/j.conbuildmat.2016.05.061

Qi, B., Gao, J., Chen, F., and Shen, D. (2017). Evaluation of the Damage Process of Recycled Aggregate concrete under Sulfate Attack and Wetting-Drying Cycles. *Constr. Build. Mater.* 138, 254–262. doi:10.1016/j.conbuildmat.2017.02.022

Sarkar, S., Mahadevan, S., Meeussen, J. C. L., van der Sloot, H., and Kosson, D. S. (2010). Numerical Simulation of Cementitious Materials Degradation under External Sulfate Attack. *Cem. Concr. Compos.* 32, 241–252. doi:10.1016/j.cemconcomp.2009.12.005

Song, K.-I., Song, J.-K., Lee, B. Y., and Yang, K.-H. (2014). Carbonation Characteristics of Alkali-Activated Blast-Furnace Slag Mortar. *Adv. Mater. Sci. Eng.* 2014, 1–11. doi:10.1155/2014/326458

Sun, X., Hua, Y., Mao, S., and Zhang, Y. (2021). Experimental Research on the Influence of Dry-Wet Cycle on Concrete Compressive Strength. *IOP Conf. Ser. Earth Environ. Sci.* 714, 032016. doi:10.1088/1755-1315/714/3/032016

Supit, S. W. M., and Shaikh, F. U. A. (2014). Durability Properties of High Volume Fly Ash concrete Containing Nano-Silica. *Mater. Struct.* 48, 2431–2445. doi:10.1617/s11527-014-0329-0

Tan, Y., Yu, H., Ma, H., Zhang, Y., and Wu, C. (2017). Study on the Micro-crack Evolution of concrete Subjected to Stress Corrosion and Magnesium Sulfate. *Constr. Build. Mater.* 141, 453–460. doi:10.1016/j.conbuildmat.2017.02.127

Vance, K., Aguayo, M., Oey, T., Sant, G., and Neithalath, N. (2013). Hydration and Strength Development in Ternary portland Cement Blends Containing limestone and Fly Ash or Metakaolin. *Cem. Concr. Compos.* 39, 93–103. doi:10.1016/j.cemconcomp.2013.03.028

Wang, J., Niu, D., Hui, H., and Wang, B. (2019). Study on Durability Degradation of Shotcrete Lining Eroded by Compound Salt. *J. Civil Eng.* 52, 79–90. doi:10.15951/j.tmgcxb.2019.09.006

Wei, J., Gencturk, B., Jain, A., and Hanifehzadeh, M. (2019). Mitigating Alkali-Silica Reaction Induced concrete Degradation through Cement Substitution by Metakaolin and Bentonite. *Appl. Clay Sci.* 182, 105257. doi:10.1016/j.clay.2019.105257

Xi, F., Davis, S. J., Ciais, P., Crawford-Brown, D., Guan, D., Pade, C., et al. (2016). Substantial Global Carbon Uptake by Cement Carbonation. *Nat. Geosci.* 9, 880–883. doi:10.1038/ngeo2840

Yuan, Q., Shi, C., De Schutter, G., Audenaert, K., and Deng, D. (2009). Chloride Binding of Cement-Based Materials Subjected to External Chloride Environment - A Review. *Constr. Build. Mater.* 23, 1–13. doi:10.1016/j.conbuildmat.2008.02.004

Zeng, J., Shui, Z., and Wang, S. (2014). Hydration and Pore Structure of Steam Cured High-Strength Mortar with Metakaolin and Slag at Early Age. *J. Cent. South Univ. (Natural Sci. Edition)* 45, 2857–2863.

Zhang, T., Wang, T., Wang, K., Xu, C., and Ye, F. (2021). Development and Characterization of NaCl-KCl/Kaolin Composites for thermal Energy Storage. *Solar Energy* 227, 468–476. doi:10.1016/j.solener.2021.09.020

Zhang, J., Tan, H., Bao, M., Liu, X., Luo, Z., and Wang, P. (2021). Low Carbon Cementitious Materials: Sodium Sulfate Activated Ultra-fine Slag/fly Ash Blends at Ambient Temperature. *J. Clean. Prod.* 280, 124363. doi:10.1016/j.jclepro.2020.124363

Zheng, S., Qi, L., He, R., Wu, J., and Wang, Z. (2021). Erosion Damage and Expansion Evolution of Interfacial Transition Zone in concrete under Dry-Wet Cycles and Sulfate Erosion. *Constr. Build. Mater.* 307, 124954. doi:10.1016/j.conbuildmat.2021.124954

Zhou, Y., Peng, Z., Chen, L., Huang, J., and Ma, T. (2021). The Influence of Two Types of Alkali Activators on the Microstructure and Performance of Supersulfated Cement concrete： Mitigating the Strength and Carbonation Resistance. *Cem. Concr. Compos.* 118, 103947. doi:10.1016/j.cemconcomp.2021.103947

Conflict of Interest: The authors declare that the research was conducted in the absence of any commercial or financial relationships that could be construed as a potential conflict of interest.

Publisher's Note: All claims expressed in this article are solely those of the authors and do not necessarily represent those of their affiliated organizations, or those of the publisher, the editors and the reviewers. Any product that may be evaluated in this article, or claim that may be made by its manufacturer, is not guaranteed or endorsed by the publisher.